Double-Diffusive Recipes. Part I: Large-Scale Dynamics of Thermohaline Staircases

Citation: Radko, T., A. Bulters, J. D. Flanagan, and J.-M. Campin. "Double-Diffusive Recipes. Part I: Large-Scale Dynamics of Thermohaline Staircases." J. Phys. Oceanogr. 44, no. 5 (May 2014): 1269–1284. © 2014 American Meteorological Society

As Published: http://dx.doi.org/10.1175/jpo-d-13-0155.1

Publisher: American Meteorological Society

Persistent URL: http://hdl.handle.net/1721.1/91958

Version: Final published version: final published article, as it appeared in a journal, conference proceedings, or other formally published context

Double-Diffusive Recipes. Part I: Large-Scale Dynamics of Thermohaline Staircases

T. RADKO, A. BULTERS, AND J. D. FLANAGAN

Department of Oceanography, Naval Postgraduate School, Monterey, California

J.-M. CAMPIN

Department of Earth, Atmospheric and Planetary Sciences, Massachusetts Institute of Technology, Cambridge, Massachusetts

(Manuscript received 8 July 2013, in final form 12 December 2013)

ABSTRACT

Three-dimensional dynamics of thermohaline staircases are investigated using a series of basin-scale staircase-resolving numerical simulations. The computational domain and forcing fields are chosen to reflect the size and structure of the North Atlantic subtropical thermocline. Salt-finger transport is parameterized using the flux-gradient formulation based on a suite of recent direct numerical simulations. Analysis of the spontaneous generation of thermohaline staircases suggests that thermohaline layering is a product of the gamma instability, associated with the variation of the flux ratio γ with the density ratio R_ρ. After their formation, numerical staircases undergo a series of merging events, which systematically increase the size of layers. Ultimately, the system evolves into a steady equilibrium state with pronounced layers 20–50 m thick. The size of the region occupied by thermohaline staircases is controlled by the competition between turbulent mixing and double diffusion. Assuming, in accordance with observations, that staircases form when the density ratio is less than the critical value of $R_{cr} \approx 1.7$, the authors arrive at an indirect estimate of the characteristic turbulent diffusivity in the subtropical thermocline.

1. Introduction

The term thermohaline staircase is used to describe a series of well-mixed layers separated by high-gradient interfaces, frequently observed in vertical temperature and salinity profiles. Thermohaline staircases represent the most dramatic manifestation of double-diffusive convection in the ocean. For finger-driven staircases, the majority of observations have come from three locations: the western tropical Atlantic (Schmitt et al. 1987, 2005), Tyrrhenian Sea (Zodiatis and Gasparini 1996), and the Mediterranean outflow in the Northeast Atlantic (Tait and Howe 1968, 1971; Magnell 1976). Common to these regions are anomalously low values of the density ratio:

$$R_\rho = \frac{\alpha T_z}{\beta S_z}, \tag{1}$$

where T_z and S_z are the vertical temperature T and salinity S gradients; and α and β are the expansion and contraction coefficients of seawater. Low values of density ratio appear to be both necessary and sufficient for staircase formation. No salt-finger staircases have been reported for $R_\rho > 2$, and the reduction of the density ratio below 1.7 is usually associated with the appearance of steplike structures in vertical T–S profiles. The spatial pattern of staircases is also highly sensitive to R_ρ. As the density ratio decreases, staircases become more pronounced and the height of steps sharply increases. This connection is significant. The density ratio is the single most important parameter controlling the intensity of salt fingers and the sensitivity of staircases to variations in R_ρ is one of many signs that staircases are a product of double diffusion.

The interest in thermohaline staircases goes well beyond intellectual curiosity. Staircases represent the obvious mixing hot spots in the main thermocline. The most extensively studied example of thermohaline layering is the Caribbean staircase, which has been the focus of two major observational programs: Caribbean-Sheets and Layers Transect (C-SALT; Schmitt et al. 1987) and

Corresponding author address: T. Radko, Department of Oceanography, Naval Postgraduate School, 833 Dyer Road, Bldg. 232, Room 328, Monterey, CA 93943.
E-mail: tradko@nps.edu

DOI: 10.1175/JPO-D-13-0155.1

Salt Finger Tracer Release Experiment (SFTRE; Schmitt et al. 2005). Tracer release and microstructure measurements in the Caribbean staircase indicate that layering increases vertical mixing by as much as an order of magnitude relative to analogous smooth-gradient regions (Schmitt et al. 2005). A critical dynamical consequence of the elevated mixing rates in the C-SALT area is the injection of salinity into the Antarctic Intermediate Water. This injection preconditions waters for later sinking in the high-latitude Atlantic, thus affecting the global thermohaline circulation. A simple estimate (R. W. Schmitt 2012, personal communication) suggests that the salt flux over a relatively small area of the Caribbean staircase exceeds the net turbulent transport due to overturning gravity waves throughout the entire North Atlantic subtropical thermocline.

Despite the persistent interest in thermohaline staircases, their dynamics are still surrounded by controversy. While the origin of staircases is undoubtedly double diffusive, specific mechanisms of layering are poorly understood and much debated. Literature on the subject contains at least half a dozen different hypotheses, as reviewed most recently by Radko (2013). For instance, Merryfield (2000) suggested that staircases represent the ultimate state of thermohaline interleaving, which is, in turn, induced by lateral temperature and salinity gradients. Radko (2003) on the other hand argued that double-diffusive layering is likely to be caused by the so-called gamma instability, which is driven by variations in the ratio of the turbulent heat and salt fluxes:

$$\gamma = \frac{\alpha F_T}{\beta F_S}. \tag{2}$$

The gamma instability hypothesis has been supported by studies based on direct numerical simulations (DNS). However, computational constraints necessarily restrict DNS modeling (e.g., Stellmach et al. 2011) to relatively small-scale phenomena ($\sim$1 m). Therefore, issues such as the influence of background lateral gradients and large-scale circulation patterns on thermohaline layering have not been properly explored. The present study attempts to address some of the unresolved problems in the theory of thermohaline staircases by means of large-scale numerical modeling.

Individual salt fingers operate on spatial scales of several centimeters, and therefore any large-scale simulation requires parameterization of finger-driven transport. However, even when salt fingers are parameterized rather than resolved, staircase modeling still represents a major challenge. Several modeling studies (Zhang et al. 1998; Merryfield et al. 1999; Oschlies et al. 2003) have already attempted to take double diffusion into account. While its inclusion affected large-scale T–S patterns, none of these simulations produced thermohaline staircases. The lack of staircases may signal that double-diffusive effects have been underestimated. Staircases are associated with the most vigorous double-diffusive mixing and therefore are more likely to be involved in large-scale dynamics than the relatively benign smooth-gradient fingering. Concerns of this nature motivate efforts to implement necessary changes in the design of models that would make staircase modeling possible.

The recipe for generating staircases in large-scale simulations is relatively simple: use high vertical resolution and add an adequate parameterization of double-diffusive mixing. To model staircases, several distinct scales must be resolved: (i) fingering interfaces ($\sim$1 m), (ii) the vertical thermocline scale ($\sim$1 km), and (iii) the lateral basin-scale circulation patterns ($\sim$1000 km). Theoretical arguments (Radko 2005) suggest that while the initial layers form rather rapidly (within weeks), the evolution and ultimate equilibration of staircases occur on the time scale of decades. Computational capabilities have only recently reached the level of resolving such a wide range of spatial and temporal scales. The second, potentially even more significant complication that has delayed the inclusion of staircases in ocean models is the uncertainty in double-diffusive parameterizations. In particular, the earlier large-scale models made no attempt to represent variation in the flux ratio. Instead, they adopted the constant flux ratio approximation, thereby a priori excluding the gamma instability from consideration.

Our study addresses both challenges by performing simulations at unprecedented vertical resolution ($\Delta z = 1$ m) and by adopting a recent parameterization of finger-induced diapycnal fluxes (Radko and Smith 2012). The Radko and Smith (2012) mixing model is based on a suite of DNS and, importantly, it reflects the systematic variation of the flux ratio with the density ratio. These modifications have proven to be essential, resulting in the first (to the best of our knowledge) large-scale staircase-resolving numerical simulation. The formation of staircases in our model is shown to be a consequence of the gamma instability. Layers that form initially are thin and unsteady. They undergo a series of merging events, in which strong interfaces, characterized by large temperature and salinity jumps, grow further at the expense of weaker interfaces that gradually erode and eventually disappear. The characteristic size of steps increases in time; the staircase eventually equilibrates when layers become sufficiently thick. The systematic analysis of merging dynamics is presented in Part II of these works (Radko et al. 2014).

The area occupied by thermohaline staircases is controlled by the competition between turbulent mixing

and double diffusion. Numerical experiments in which diapycnal mixing is predominantly double diffusive are characterized by the spreading of staircases throughout the model domain. When the strengths of double-diffusive and turbulent mixing are comparable, staircases are localized in a southern region of the basin—the counterpart of the C-SALT area in the North Atlantic. When the turbulent diffusivity exceeds that of double diffusion, staircases do not form. The behavior observed in the numerical simulations is rationalized by a simple analytical model, which links staircase area with the intensity of turbulent mixing. The model is then used to infer the characteristic values of turbulent diffusivity in the main thermocline based on the observed incidence of layering in the ocean.

This manuscript is organized as follows: In section 2, we describe the model setup and present preliminary numerical experiments, illustrating the tendency of finger favorable, initially smooth stratification to evolve into well-defined staircases. The layering observed in simulations is attributed to the gamma instability effect, which is reviewed in section 3. The analytical model (section 3) is extended to explore the sensitivity of staircases to the assumed level of the background turbulent mixing K^{turb}. In section 4, theoretical arguments are validated by a suite of simulations in which K^{turb} is systematically varied. Section 5 describes the evolutionary pattern of newly generated layers. We summarize and discuss our findings in section 6.

2. Formulation

We solve the incompressible Boussinesq equations in a rotating frame using the Massachusetts Institute of Technology General Circulation Model (MITgcm)—a finite volume numerical model described in Marshall et al. (1997a,b). Computations are carried out in a rectangular domain with dimensions of $(L_x, L_y, L_z) = (6400\,\text{km}, 3200\,\text{km}, 4000\,\text{m})$, using a Cartesian grid with $64 \times 32 \times 1003$ elements. The thermocline ($-1000 < z < 0\,\text{m}$) is resolved by 1000 grid points in z ($\Delta z = 1\,\text{m}$), and only 3 points ($\Delta z = 1\,\text{km}$) are used for the abyssal region ($-4000 < z < -1000\,\text{m}$). The model is designed to reflect the general structure of the North Atlantic subtropical thermocline, and the system is forced by a zonal wind stress:

$$\tau = -\tau_0 \cos\left(\pi \frac{y}{L_y}\right) + \tau_1, \quad 0 < y < L_y, \tag{3}$$

where $\tau_0 = 0.055\,\text{N m}^{-2}$ and $\tau_1 = 0.015\,\text{N m}^{-2}$. The variation in the Coriolis parameter f is represented by the beta-plane approximation

$$f = f_0 + \beta_c y, \tag{4}$$

where $f_0 = 2.5 \times 10^{-5}\,\text{s}^{-1}$ and $\beta_c = 10^{-11}\,\text{m}^{-1}\,\text{s}^{-1}$.

In addition, thermohaline forcing is applied by weakly relaxing the surface temperature and salinity to the zonally uniform target patterns shown in Figs. 1a and 1b. The abyssal values are relaxed to $T_{\text{abyss}} = 4.7°\text{C}$ and $S_{\text{abyss}} = 34.1$. Temperature and salinity are also relaxed to the prescribed (linear) patterns at the northern boundary ($y = L_y$) of the thermocline region. Such choice of the forcing patterns represents a conventional and physically motivated (Luyten et al. 1983) setup of the subtropical thermocline problem. The corresponding target thermocline density ratio

$$R_{\rho_{\text{net}}} = \frac{\alpha(T_{z=0} - T_{\text{abyss}})}{\beta(S_{z=0} - S_{\text{abyss}})} \tag{5}$$

linearly increases from $R_{\rho_{\text{net}}} = 1.5$ at $y = 0$ to $R_{\rho_{\text{net}}} = 2.4$ at $y = L_y$ (Fig. 1c). The chosen patterns are qualitatively consistent with the observed (Levitus and Boyer 1994) temperature and salinity distribution in the North Atlantic subtropical thermocline. The lateral dissipation of the momentum and tracers by unresolved scales of motion is represented by horizontal eddy viscosity $A_H = 1.6 \times 10^5\,\text{m}^2\,\text{s}^{-1}$ and diffusivity $K_H = 500\,\text{m}^2\,\text{s}^{-1}$.

The vertical mixing in the model contains three distinct components. For our purpose, the most significant contributor is double diffusion. The diffusivities of temperature and salinity (K_T^{dd}, K_S^{dd}) are parameterized using the closure proposed by Radko and Smith (2012) on the basis of salt-finger DNS:

$$K_T^{\text{dd}} = F_S k_T \gamma \quad \text{and} \quad K_S^{\text{dd}} = F_S k_T R_\rho, \tag{6}$$

where $k_T = 1.4 \times 10^{-7}\,\text{m}^2\,\text{s}^{-1}$ is the molecular diffusivity of heat and

$$\begin{cases} F_S = \dfrac{a_S}{\sqrt{R_\rho - 1}} + b_S, \quad (a_S, b_S) = (135.7, -62.75) \\ \gamma = a_\gamma \exp(-b_\gamma R_\rho) + c_\gamma, \quad (a_\gamma, b_\gamma, c_\gamma) = (2.709, 2.513, 0.5128). \end{cases} \tag{7}$$

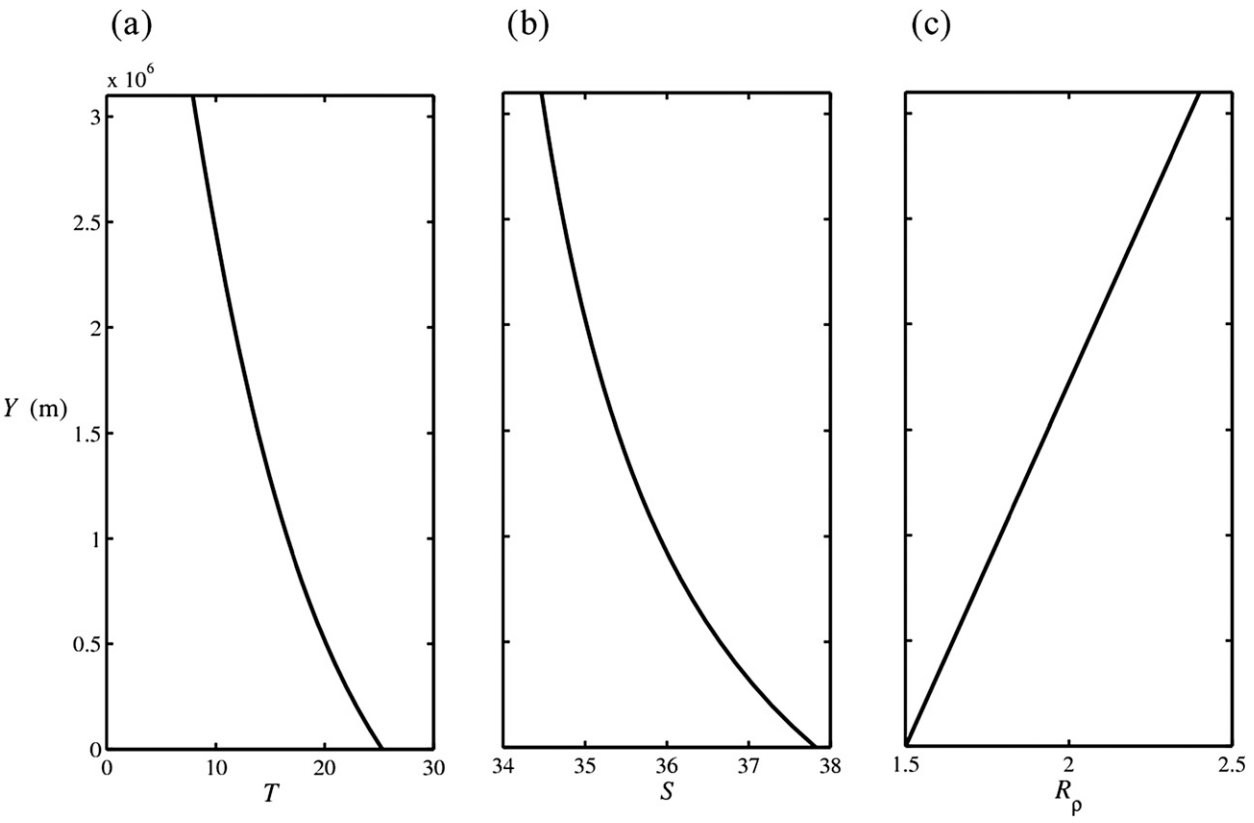

FIG. 1. The target (a) sea surface temperature and (b) salinity patterns. (c) Also shown is the pattern of the net target density ratio (5) across the model thermocline.

The parameterization (6)–(7) was derived using simulations in the range $1 < R_\rho < 3$. The flux pattern for $R_\rho > 3$ is of secondary importance because, in this regime, finger-induced transport is weak and has virtually no impact on the large-scale dynamics. In terms of implementation in the MITgcm, the foregoing parameterization is used for $R_\rho < R_{\text{cutoff}}$, where $R_{\text{cutoff}} = 5.67$ is the point at which parameterized diffusivities (6)–(7) reduce to zero. For $R_\rho > R_{\text{cutoff}}$, we assign $K_T^{\text{dd}} = K_S^{\text{dd}} = 0$.

The second contributor to the vertical transport is turbulent diffusion. For simplicity, the turbulent diffusivity K^{turb} in the thermocline interior, associated with overturning gravity waves, is assumed to be spatially uniform and equal for temperature and salinity. In a series of experiments performed in this study, K^{turb} is systematically varied from 0 to $10^{-5}\,\text{m}^2\,\text{s}^{-1}$ with the remainder of this section describing experiments performed with $K^{\text{turb}} = 1.35 \times 10^{-6}\,\text{m}^2\,\text{s}^{-1}$. The surface mixed layer turbulence is represented using the K-profile parameterization (KPP) model (Large et al. 1994), and the convective adjustment scheme is used for the hydrostatically unstable regions. Finally, the vertical mixing scheme is supplemented by biharmonic diffusion, represented by the terms $K_4(\partial^4 T/\partial z^4)$ and $K_4(\partial^4 S/\partial z^4)$ in the advection–diffusion T–S equations. The reason for including biharmonic diffusion is related to the ultraviolet catastrophe of double-diffusive flux-gradient laws—the growth rate of unstable perturbations increases without bound as the vertical wavelength decreases to zero. This ultraviolet catastrophe is unphysical because the flux-gradient flux laws themselves are valid only for scales that greatly exceed the characteristic salt-finger width [see the discussion in Radko (2005)]. The associated numerical complications are surmounted by including biharmonic terms, which selectively damp small (i.e., comparable to the grid spacing) scales but have little effect on longer wavelengths.

An important ramification of the inclusion of biharmonic diffusion in the model is our ability to control the thickness of high-gradient interfaces. Our ongoing research activities (Radko 2014, manuscript submitted to *J. Fluid Mech.*) suggest that in DNS, and perhaps in nature as well, the interfacial thickness is determined by the point-of-failure scale—the minimal vertical scale at which the flux-gradient laws offer an adequate description of vertical transport. In our large-scale parametric model, the scale of interfaces is set by the biharmonic diffusivity. This addition makes it possible

to represent, however crudely, the point-of-failure effect. When biharmonic diffusion is not employed ($K_4 = 0$) the thickness of all interfaces inexorably reduces to the minimal-resolved scale of one grid point $h = \Delta z = 1$ m. Although such thin interfaces have been observed in the C-SALT staircase, they are poorly represented by the computational grid. Some trial-and-error experimentation led us to choose $K_4 = 5 \times 10^{-6}\,\mathrm{m^4\,s^{-1}}$ for the following simulations, which results in interfaces of $h \approx 2 - 5$ m. Interfaces of such height are also common (Schmitt et al. 1987) and are reasonably well represented by the numerical model.

The integrations were initiated with the ocean at rest. The initial vertical stratification is linear throughout the thermocline ($-1000 < z < 0$ m), matching the surface (Figs. 1a,b) and abyssal values of temperature and salinity. For each set of parameters, simulations were carried out for 70 yr, which is sufficient for the equilibration of the model thermocline. The time step was $\Delta t = 400$ s, and the restoring time scale at the surface, in the abyss, and at the northern boundary was set to 12 h. The overall structure of the resulting flow field reflects all major dynamic features expected for subtropical gyres. The typical circulation pattern (Fig. 2a) consists of a Sverdrup-type interior flow bounded on the west by a narrow intensification region. The thermocline tends to deepen from east to west in the interior, reaching the maximum depth at the seaward edge of the western boundary current and then shallows toward the western boundary (Fig. 2b). The general structure of the circulation pattern, the overall distribution of temperature and salinity, and the typical magnitudes of large-scale T–S gradients (vertical and horizontal) remain similar in all experiments considered in this study.

The novel feature of the presented experiments is the spontaneous formation of well-defined thermohaline staircases, exemplified by the vertical temperature and salinity profiles in Fig. 3. These profiles represent a series of mixed layers separated by high-gradient interfaces, suggestive of the typical oceanographic observations (e.g., Schmitt et al. 2005). The step heights in the model staircases are highly variable, ranging from 10 to 150 m, although most steps are limited to 20–50 m. Figure 4 presents three-dimensional visualizations of the temperature gradient field in the southwestern region of the computational domain (the model counterpart of the C-SALT area). The staircases initially form on a time scale of years (depending on the location) and subsequently undergo a series of merging events. The typical step size of the staircase in Fig. 4b ($t = 5$ yr) is considerably less than that at $t = 20$ yr in Fig. 4c. The extension of the model run to $t = 70$ yr (not shown) resulted in only minimal changes in the staircase pattern.

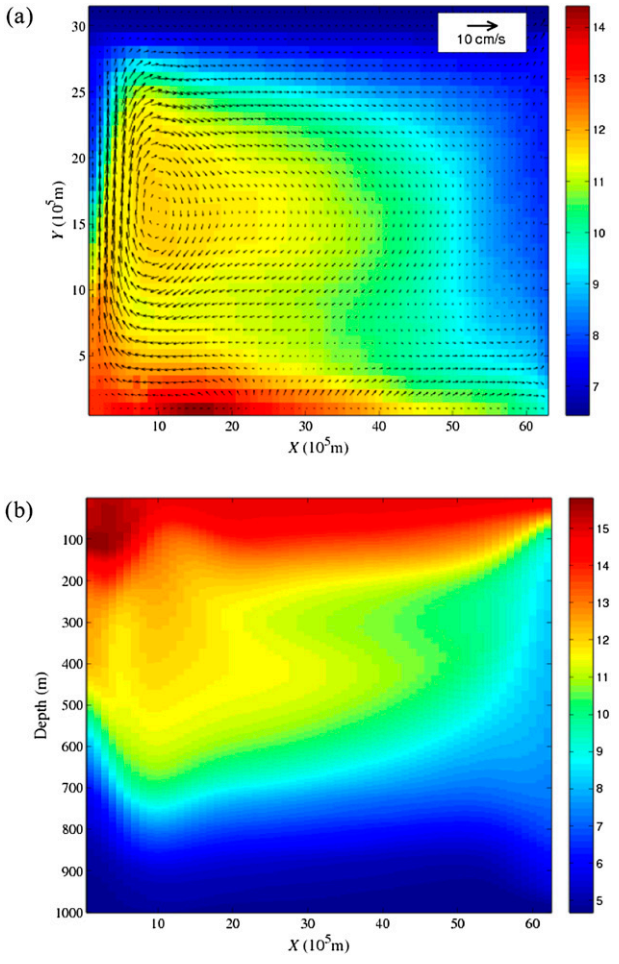

FIG. 2. The circulation pattern and temperature distribution after 70 yr of integration. (a) Horizontal section at the center of the model thermocline ($z = -0.5L_z$). (b) Vertical section at $y = 0.5L_y$.

This suggests that 2 decades is the typical time scale for the evolution and eventual equilibration of thermohaline staircases of the C-SALT class. The simulation in Fig. 4 reveals a complex three-dimensional topology of interfaces, with numerous instances of interfaces terminating in space, coalescing with other interfaces, and changing their spatial orientation.

One of the central questions addressed by this study concerns the origin of staircases. An important clue is brought by the comparison of three experiments shown in Fig. 5. These experiments are identical in all respects except for the chosen model of diapycnal mixing. The simulation in Fig. 5a has been performed with the double-diffusive parameterization (7) used throughout this study. A seemingly subtle modification was made in Fig. 5b: the flux ratio was set to a constant by assuming $\gamma = c_\gamma = 0.5128$ instead of the expression in (7). Finally, the simulation in Fig. 5c has been performed without

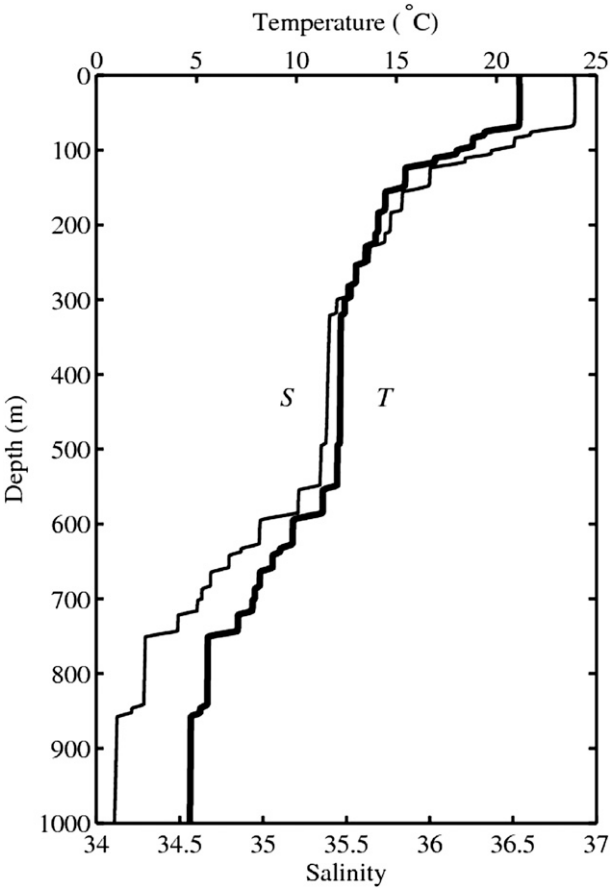

FIG. 3. Typical vertical distribution of temperature and salinity in the staircase region of the thermocline. The profiles were taken at $(x, y) = (500\,\text{km}, 500\,\text{km})$ after 70 yr of integration.

double-diffusive mixing ($K_T^{dd} = K_S^{dd} = 0$). While the large-scale temperature patterns in all three experiments are similar, only the first experiment, incorporating the variable flux ratio model, produced a thermohaline staircase. Based on the stark difference in the outcome, we conclude that (i) layer formation is fundamentally double diffusive, and (ii) the mechanism of layering is associated with the variation of the flux ratio with the density ratio. The latter proposition is consistent with the gamma instability theory of layer formation, which is discussed and extended next.

3. Gamma instability mechanism

Theoretical arguments and diagnostics of salt-finger DNS (Walsh and Ruddick 2000; Radko 2003; Stellmach et al. 2011) suggest that uniform vertical fingering-favorable stratification is unstable as long as the flux ratio γ decreases with the density ratio R_ρ. This condition is met for relatively low values of R_ρ. The $\gamma(R_\rho)$ relation over the full range of instability ($1 < R_\rho < \tau^{-1} \sim 100$, where $\tau \approx 0.01$ is the molecular salt/heat diffusivity ratio) can be inferred, for instance, from linear stability analysis (Schmitt 1979a). This pattern is shown schematically in Fig. 6a. Schmitt's model suggests that, as R_ρ increases from unity, γ first decreases, reaches a minimum at $R_{min} \approx 4$, and then gradually increases. Laboratory experiments (e.g., Schmitt 1979b) and DNS (e.g., Traxler et al. 2011) confirm that, in the absence of any non-double-diffusive mixing processes, γ decreases with R_ρ everywhere in the range $1 < R_\rho < 4$. The resulting gamma instability takes the form of horizontally uniform perturbations, which grow monotonically and eventually transform the initial smooth gradient into a series of convecting layers separated by high-gradient interfaces, as shown in the schematic in Fig. 6b. However, the gamma instability argument, combined with the decrease in γ for $1 < R_\rho < 4$ seems to suggest that thermohaline staircases are bound to form over most of the Atlantic thermocline, which is inconsistent with observations. One of the goals of the present study is to find a plausible resolution of the staircase conundrum.

The original argument and numerical tests of the gamma instability theory were made for mixing driven entirely by salt fingers. However, a little reflection suggests that the effect can be immediately generalized to the more realistic case in which diapycnal mixing includes the contribution from wave-induced turbulence and from molecular diffusion. The instability condition in this case becomes

$$\frac{\partial \gamma_{tot}}{\partial R_\rho} < 0, \tag{8}$$

where

$$\gamma_{tot} = \frac{K_T^{dd} + K^{turb} + k_T}{K_S^{dd} + K^{turb} + k_S} R_\rho. \tag{9}$$

It is indicated in (8) and (9) that K^{turb} directly affects the pattern of the total flux ratio and thereby influences the gamma instability conditions. Thus, a possible answer to the staircase conundrum is that the inclusion of turbulent wave-induced mixing reduces the unstable density ratios to a more narrow range of $1 < R_\rho < 1.7$ suggested by observations (e.g., Schmitt et al. 1987).

The calculations in Fig. 7 tend to support this proposition. Here, we plot the total flux ratio as a function of density ratio for various values of K^{turb}. Turbulent diffusivity in the main thermocline is still poorly constrained by field measurements, but it is likely to be on the order of $K^{turb} \sim 10^{-6} - 10^{-5}\,\text{m}^2\,\text{s}^{-1}$. The inclusion of

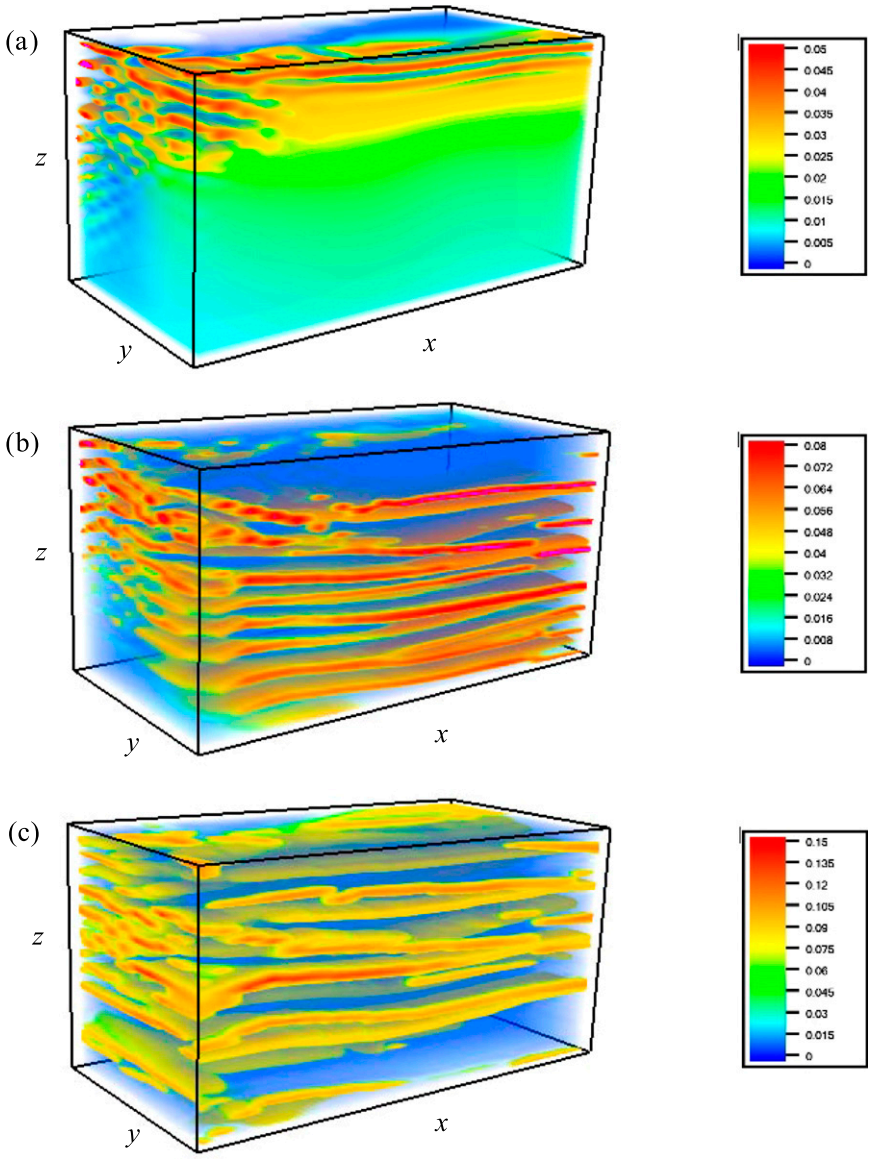

FIG. 4. Three-dimensional rendering of the vertical temperature gradient T_z °C m^{-1} in a rectangular region located in the upper-southwestern thermocline ($500 < x < 2500$ km, $500 < y < 1500$ km, and $-300 < z < -150$ m). The temperature gradient patterns after (a) 2, (b) 5, and (c) 20 yr of integration are shown.

turbulent mixing, even at such low levels, produces major changes to the $\gamma_{\rm tot}(R_\rho)$ pattern. For $K^{\rm turb} = 10^{-5}$ m^2 s^{-1}, the flux ratio monotonically increases with increasing R_ρ. Hence, the smooth-gradient stratification is linearly stable and no staircases are expected to form. The reduction of turbulent diffusivity to $K^{\rm turb} = 5 \times 10^{-6}$ m^2 s^{-1} makes the $\gamma_{\rm tot}(R_\rho)$ relation slightly nonmonotonic (Fig. 7). However, the unstable region is limited to unrealistically low values of density ratio ($R_\rho < 1.3$). The observationally inferred layering condition for the C-SALT staircase ($R_\rho < 1.7$) is met for

$$K^{\rm turb} = 1.35 \times 10^{-6}\ {\rm m^2\ s^{-1}}. \qquad (10)$$

The estimate (10) is generally consistent with observational assessments of wave-induced mixing based on microstructure measurements and on finescale parameterizations (e.g., Gregg 1989; Polzin et al. 1995). For the low-latitude C-SALT region, parameterization of mixing supported by the background internal wave field (Schmitt et al. 2005) suggests a diffusivity of $K^{\rm turb} \sim 2 \times 10^{-6}$ m^2 s^{-1}, only slightly exceeding our indirect inference.

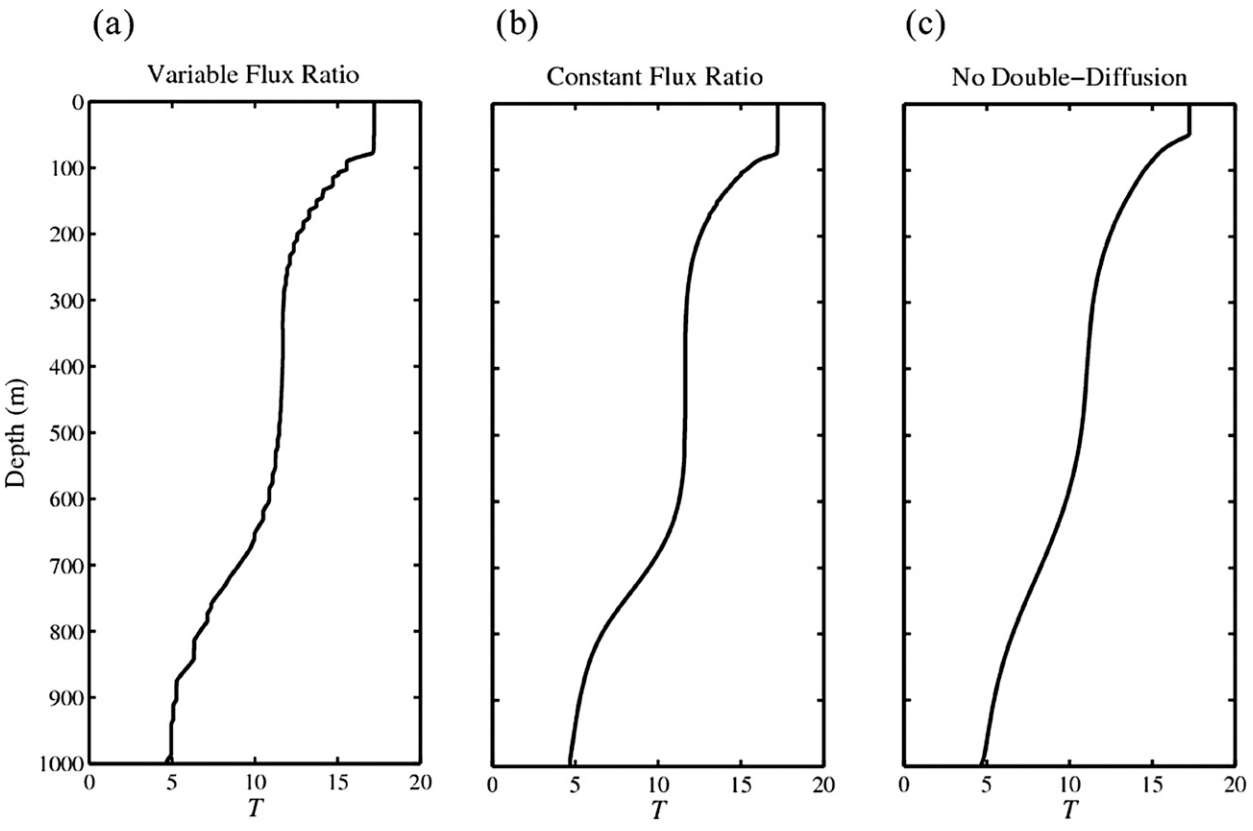

FIG. 5. Origin of staircases. The vertical temperature profiles at $(x, y) = (1000\,\text{km}, 1000\,\text{km})$ in the experiments with (a) the double-diffusive mixing model based on the variable flux ratio parameterization, (b) the double-diffusive model based on the uniform flux ratio parameterization, and (c) the turbulent mixing model. Only the experiment in (a) resulted in the formation of thermohaline staircases.

It is also of interest to examine the effects of molecular diffusion on layering conditions. Therefore, in Fig. 7 we compare the flux ratio pattern that does not take molecular diffusion into account (heavy curve in Fig. 7) with the one that does (dashed curve). Both calculations assume turbulent diffusivity in (10). The difference in the patterns is small but detectable. The inclusion of molecular transport with $(k_T, \tau) = (1.38 \times 10^{-7}, 0.01)$ slightly increases the flux ratio and shifts its minimum from $R_{\min} = 1.7$ to $R_{\min} = 1.66$.

To quantify the link between spontaneous layering and the intensity of turbulent mixing, in Fig. 8 we plot the layering threshold $R_{\min}$ as a function of turbulent diffusivity K^{turb}. This function can be accurately approximated by the linear/logarithmic relation:

$$\log_{10}(K^{\text{turb}}) = -1.32R_{\min} - 3.62. \qquad (11)$$

Note that the threshold density ratio in thermohaline staircases can be easily inferred from hydrographic measurements. On the other hand, the evaluation of turbulent diffusivity from microstructure data is subject to substantial errors, particularly for the mixed (double diffusive/turbulent) environment. Therefore, the significance of relation (11) lies in the simple, albeit indirect, method it provides for estimating the background turbulent diffusivity in the vicinity of thermohaline staircases in the World Ocean.

4. The staircase region: Effects of turbulent mixing

An obvious limitation of the gamma instability theory is related to its idealized one-dimensional character. The analytical model does not take into account the effects of lateral temperature and salinity gradients, advection by large-scale shears, and spatial nonuniformity of the background vertical stratification—all of which are omnipresent in the ocean. The large-scale numerical simulations described in section 2 afford the opportunity to test the predictive capabilities of the gamma instability theory in a three-dimensional setting.

To determine whether layering conditions based on the gamma instability theory match the incidences of staircase formation in the numerical model, we consider a set of four large-scale experiments set up in the manner described in section 2. The only difference between

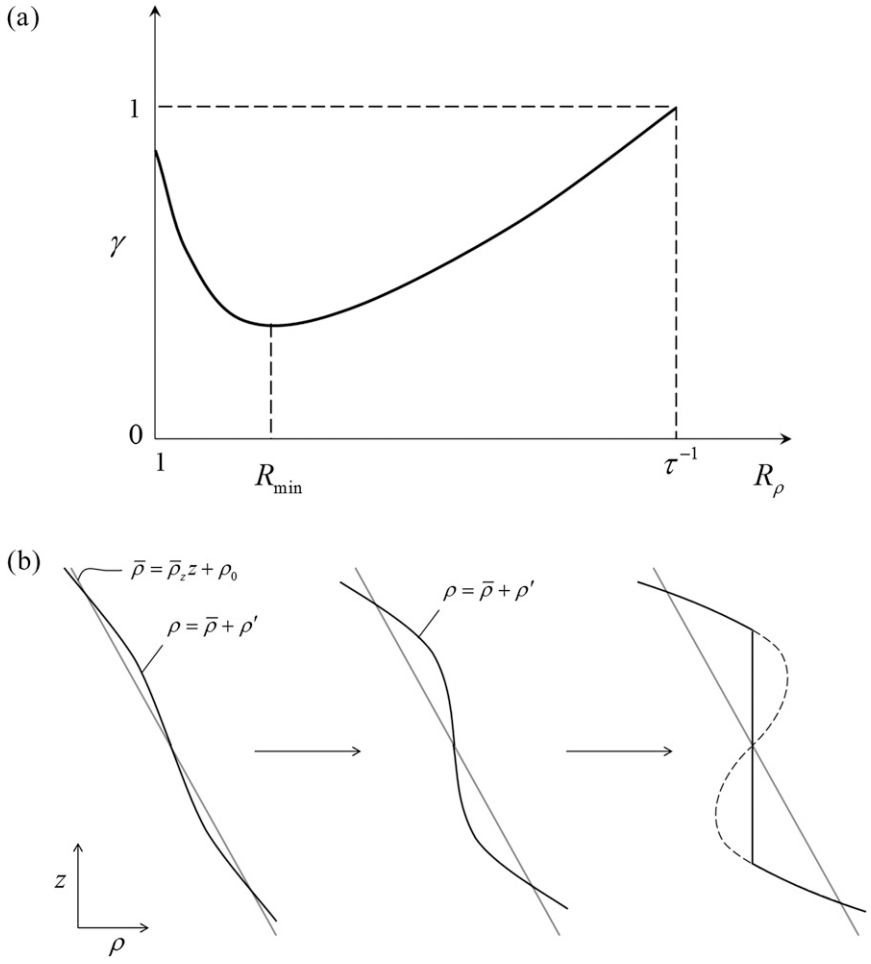

FIG. 6. The gamma instability theory of double-diffusive layering. (a) Dependence of the flux ratio on the density ratio in fingering convection. The flow in the parameter range $1 < R_\rho < R_{min}$ is susceptible to the gamma instability. (b) The monotonic amplification of the horizontally uniform gamma instability modes transforms the initially uniform stratification into a series of convecting layers separated by high-gradient interfaces.

the experiments is in the chosen values of turbulent diffusivity—$K^{turb} = 0$, 1.35×10^{-6}, 3×10^{-6}, and $10^{-5}\,m^2\,s^{-1}$. Because the density ratio varies considerably in the vertical, whereas layering is likely to be controlled by local conditions, we focus our analysis on a relatively narrow region located at the center of the model thermocline between 450 and 550 m. The density ratio there is defined accordingly as

$$R_{\rho_{500}} = \frac{\alpha(T|_{z=-450\,m} - T|_{z=-550\,m})}{\beta(S|_{z=-450\,m} - S|_{z=-550\,m})}. \qquad (12)$$

In Fig. 9, the pattern of $R_{\rho_{500}}$ at the end of each experiment ($t = 70$ yr) is plotted along with the staircase area (indicated by gray shading). The operational definition for the presence/absence of staircases in the numerical model is based on the abundance of well-mixed interior layers. In these diagnostics, a mixed layer is defined as a region where the local density gradient is less than 10% of the overall gradient between 450 and 550 m.

For each experiment, the staircase areas are compared with the corresponding predictions based on the gamma instability theory ($R_\rho < R_{min}$). The contours $R_{\rho_{500}} = R_{min}$, bounding the theoretically predicted staircase regions, are indicated by the heavy curves. The calculations in Fig. 9 indicate that the gamma instability theory is consistent with simulated layering. As anticipated, for $K^{turb} = 0$ (Fig. 9a) staircases spread throughout the model domain, whereas for $K^{turb} = 10^{-5}\,m^2\,s^{-1}$ (Fig. 9d) staircases do not form. For the intermediate cases of $K^{turb} = 1.35 \times 10^{-6}\,m^2\,s^{-1}$ (Fig. 9b) and $K^{turb} = 3 \times 10^{-6}\,m^2\,s^{-1}$ (Fig. 9c), the boundaries of the staircase

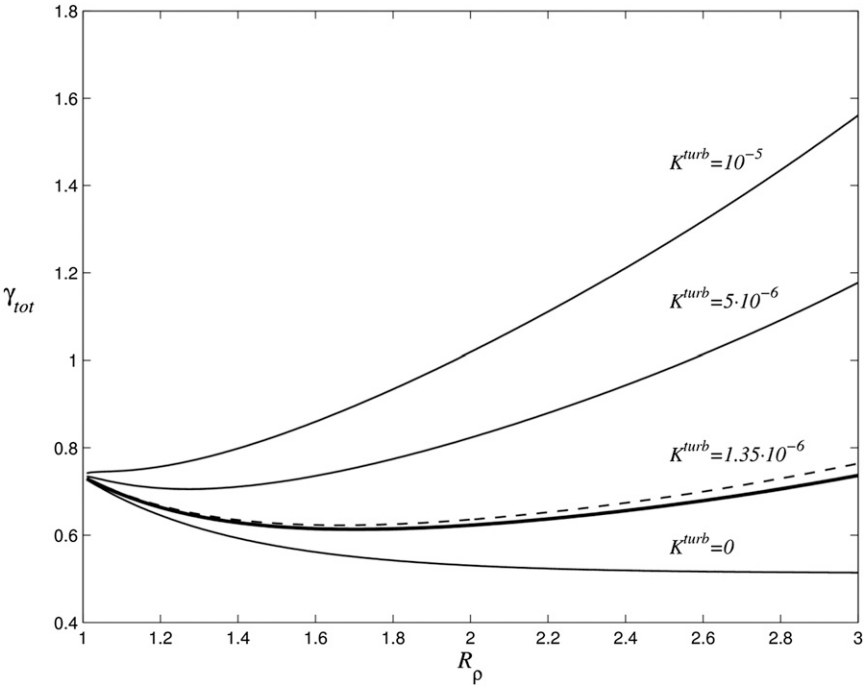

FIG. 7. Effect of turbulent mixing on the pattern of the $\gamma(R_\rho)$ relation. An increase in turbulent diffusivity K^{turb} shifts the location of the flux ratio minimum R_{min} to lower density ratios, which reduces the parameter range affected by the gamma instability ($1 < R_\rho < R_{\text{min}}$). The calculations indicated by the heavy solid and dashed curves use the same turbulent diffusivity $K^{\text{turb}} = 1.35 \times 10^{-6}\ \text{m}^2\ \text{s}^{-1}$; however, the former excludes the molecular contribution and the latter includes it. The calculations indicated by thin solid curves do not include the molecular diffusion.

regions generally follow the R_{min} contours. The agreement suggests that the zero-order dynamics of layer formation in the ocean is adequately captured by the one-dimensional gamma instability model. In the present coarse-resolution experiments, lateral variability and large-scale advection play only secondary roles in the formation of numerical staircases. It remains to be seen to what extent this conclusion holds in eddy-resolving simulations, allowing for much higher and more realistic lateral variability.

With regard to the location of staircases in Fig. 9, it should be mentioned that the layering-favorable conditions in the Caribbean are at least partially attributable to the northward transport of relatively cold and fresh Antarctic Intermediate Water. This flow results in the local reduction of R_ρ below 1.7 in the C-SALT region. Although this water mass is not present in the idealized model presented here, the corresponding distribution of R_ρ is maintained by relaxing the surface temperature and salinity to the target patterns (Fig. 1), which are progressively more layering favorable toward the south. The predominantly anticyclonic wind-driven circulation shifts the southern low-R_ρ zone to the west. This, in turn, produces the staircase in the southwestern part of the basin for moderate values of K^{turb} (Figs. 9b,c).

It is also of interest to note the sensitivity of the density ratio distribution in Fig. 9 to the assumed form of vertical mixing. The simulations with finger-dominated mixing (Figs. 9a,b) resulted in substantially lower values of the midthermocline density ratios than their turbulence-dominated counterparts (Figs. 9c,d). Thus, once double diffusion is initiated, it tends to create even more favorable conditions for its maintenance. This somewhat counterintuitive effect appears to be robust and has also been noted in earlier simulations that did not resolve thermohaline staircases (Merryfield et al. 1999).

While changes in the assumed mixing parameterization elicit the strongest response in terms of the density ratio pattern, the presence/absence of staircases and double diffusion significantly affects other key characteristics of the model thermocline. In Table 1, we list the following integral quantities realized in the final equilibrated state of each experiment. The average (indicated by angle brackets) midlevel buoyancy frequency is defined as

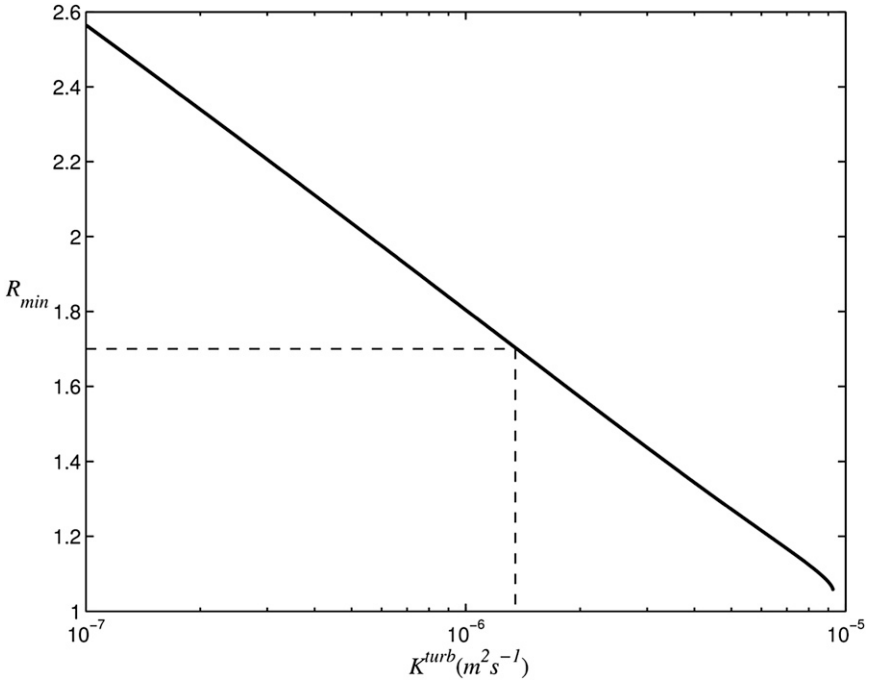

FIG. 8. The threshold density ratio for layering $R_{\min}$ as a function of turbulent diffusivity K^{turb}. Dashed lines indicate the critical density ratio for layering in the Caribbean staircase ($R_\rho = 1.7$) and the corresponding turbulent diffusivity of $K^{\text{turb}} = 1.35 \times 10^{-6}\,\text{m}^2\,\text{s}^{-1}$.

$$\langle N_{500} \rangle = \sqrt{g(\beta \Delta S_{500} - \alpha \Delta T_{500})/\Delta H}, \tag{13}$$

where $\Delta T_{500} = \overline{T}_{z=-450\,\text{m}} - \overline{T}_{z=-550\,\text{m}}$, $\Delta S_{500} = \overline{S}_{z=-450\,\text{m}} - \overline{S}_{z=-550\,\text{m}}$ (bars denote horizontal averages), and $\Delta H = 100\,\text{m}$. There is a general tendency for $\langle N_{500} \rangle$ to decrease when double diffusion is most active. The average density ratio in Table 1 is

$$\langle R_{\rho_{500}} \rangle = \frac{\alpha \Delta T_{500}}{\beta \Delta S_{500}}, \tag{14}$$

and it is significantly reduced when mixing is dominated by double diffusion. The local thermocline depth $H_{\text{therm}}(x, y)$ is defined by the point where density equals $\rho_{\text{therm}} = 0.5(\overline{\rho}_{z=0} + \rho_{\text{abyss}})$. It is then averaged in x and y and listed in Table 1 ($\overline{H}_{\text{therm}}$). The thermocline is most shallow when double diffusion is dominant and staircases spread throughout the model domain. The last two columns list the basin-integrated heat content anomaly

$$\text{HC} = \rho c_p \int_V (T - T_{\text{abyss}})\, dV, \tag{15}$$

where $c_p = 4000\,\text{J}\,(\text{kg}\,^\circ\text{C})^{-1}$, and the corresponding salt content anomaly

$$\text{SC} = \int_V (S - S_{\text{abyss}})\, dV, \tag{16}$$

both of which are elevated in the runs with predominantly double-diffusive mixing.

5. Layer-merging events

The gamma instability theory predicts that the initially formed layers are relatively thin and unsteady. The propensity for the initial dominance of small-scale steps is a consequence of the aforementioned (section 2) ultraviolet catastrophe of the flux-gradient laws—small perturbations grow faster than large ones. However, the gamma instability model assumes from the outset a certain scale separation between layering modes and salt fingers, and therefore it applies only to sufficiently long wavelengths. While the range of validity of the flux-gradient laws cannot be deduced internally from the gamma instability theory, simulations (Traxler et al. 2011; Stellmach et al. 2011) indicate that scales exceeding salt-finger width by an order of magnitude or more are accurately represented by the model; smaller scales are not. Thus, the largest growth rates are expected to occur in the vicinity of the point-of-failure scale of the flux-gradient model. The DNS of Stellmach

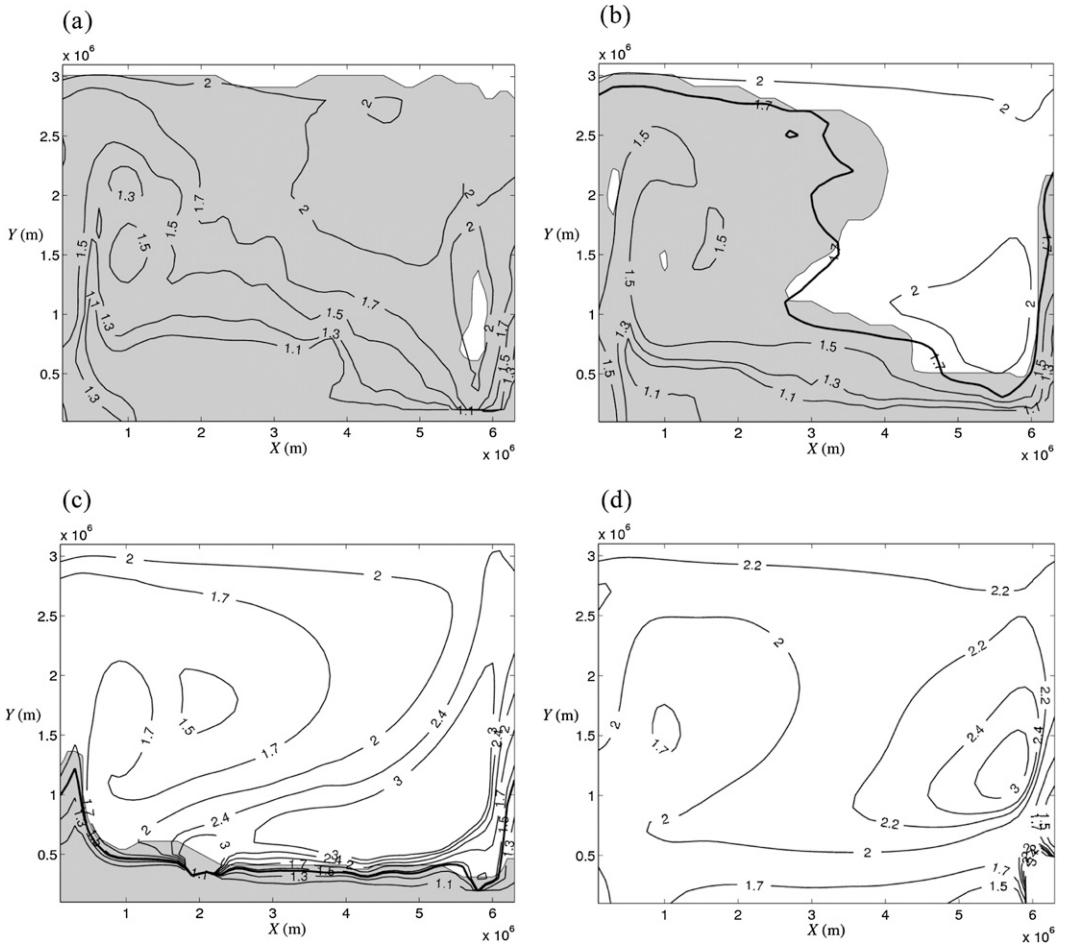

FIG. 9. The areas occupied by thermohaline staircases (shaded regions) are plotted along with the density ratio contours. These quantities are evaluated over the depth range $-550 < z < -450$ m. Theoretically predicted values of the threshold density ratio $R_{\min}$ are indicated by heavy curves. Numerical experiments with K^{turb} equal to (a) 0, (b) 1.35×10^{-6}, (c) 3×10^{-6}, and (d) $10^{-5}\,\text{m}^2\,\text{s}^{-1}$ are shown.

et al. (2011) reveal that the wavelength of the gamma instability mode destined to evolve into the initial staircase exceeds the typical horizontal wavelength of salt fingers by a factor of 20. For typical stratification of the midlatitude thermocline, this translates to the initial layer thickness of 1–2 m. This suggestion appears to be at odds with oceanographic observations of much thicker steps of 10–100 m, which are more common in salt-finger staircases.

DNS have offered an important hint for the step-size selection puzzle. While the layers that formed first are relatively thin, shortly after their appearance they start to merge sequentially. There is a general tendency for strong steps characterized by significant temperature

TABLE 1. Summary of the key integral characteristics of the final state realized in each experiment (see the text). Note the sensitivity of the thermocline structure to the chosen mixing model.

Expt	Description	$\langle N_{500}\rangle$ ($10^{-3}\,\text{s}^{-1}$)	$\langle R_{\rho_{500}}\rangle$	$\overline{H}_{\text{therm}}$ (m)	HC (10^{23} J)	SC (10^{16} psu m^3)
ExptND	No double diffusion	2.85	2.21	459	3.08	1.01
ExptCD	Constant γ	2.10	2.15	432	3.64	1.44
Expt1	$K^{\text{turb}} = 0$	2.20	1.72	424	3.46	1.32
Expt2	$K^{\text{turb}} = 1.35 \times 10^{-6}\,\text{m}^2\,\text{s}^{-1}$	2.26	1.68	431	3.50	1.34
Expt3	$K^{\text{turb}} = 3 \times 10^{-6}\,\text{m}^2\,\text{s}^{-1}$	2.18	1.86	449	3.57	1.36
Expt4	$K^{\text{turb}} = 10^{-5}\,\text{m}^2\,\text{s}^{-1}$	2.73	2.00	450	3.31	1.18

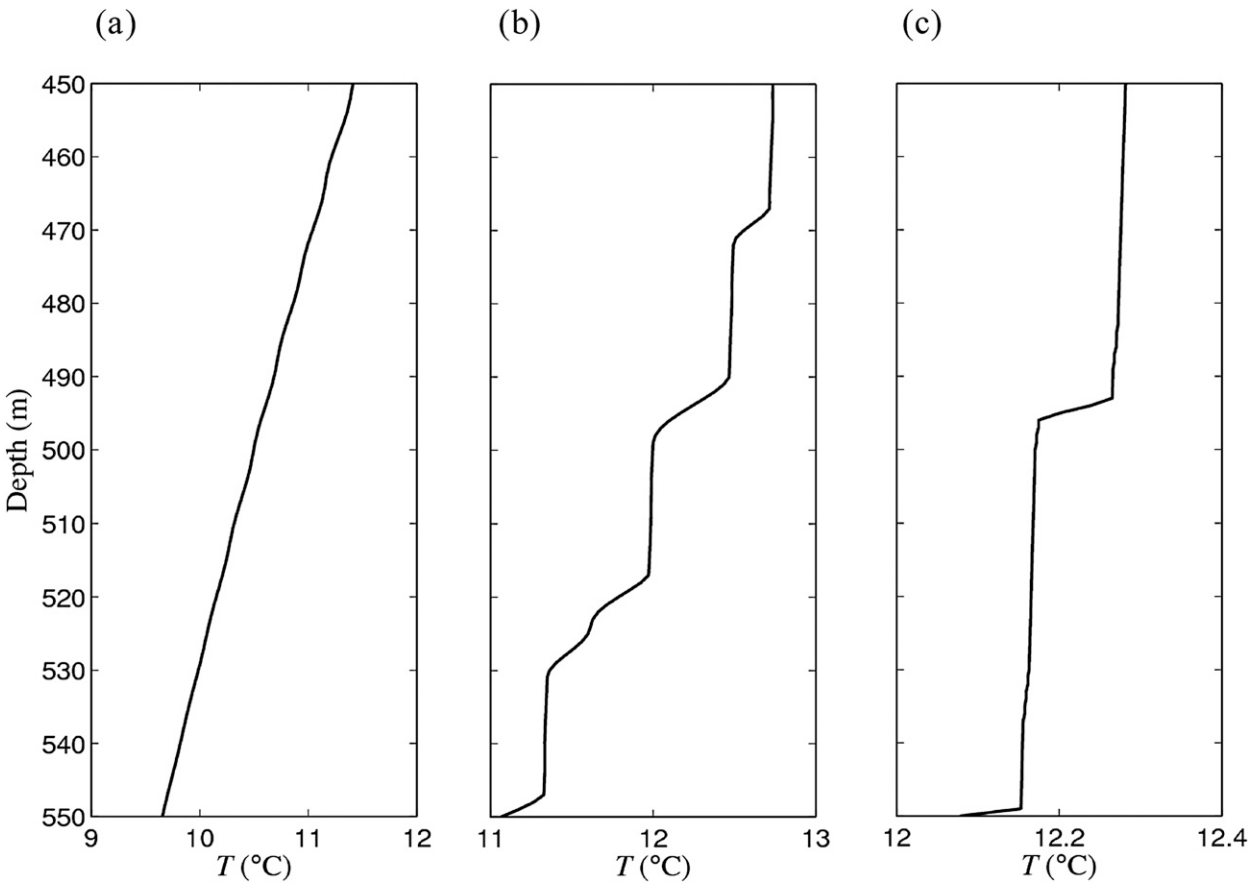

FIG. 10. Formation and evolution of layers. The vertical temperature profiles are shown at t equal to (a) 5, (b) 20, and (c) 40 yr. The appearance of well-mixed layers separated by thin stratified interfaces is followed by a series of merging events.

and salinity jumps to grow further at the expense of weaker steps, which gradually erode and eventually disappear. This merging pattern is referred to as the "B merger" mode in the classification of Radko (2007)—in contrast to the "H merger" scenario in which high-gradient interfaces drift vertically and coalesce with the adjacent interfaces. An interesting and rare example of the observed evolution of an oceanic staircase was presented by Zodiatis and Gasparini (1996), who documented changes in the Tyrrhenian Sea staircase over the course of 2 decades. This staircase contained 10 layers in the 1973 T–S profiles. However, only four spectacular layers several hundred meters thick remained present at the same location in 1992 measurements. Inspection of the incremental changes in stratification suggests that the coarsening of the Tyrrhenian staircase was caused by the B-type merging events.

Given the generic tendency of staircases to coarsen prior to their eventual equilibration—as revealed by DNS, theoretical arguments, and even some observations—it is of interest to determine whether the same evolutionary patterns are realized in our parametric large-scale model. Figure 10 presents a sequence of temperature profiles (from the $K^{\text{turb}} = 1.35 \times 10^{-6}\ \text{m}^2\ \text{s}^{-1}$ experiment) at $(x, y) = (500\ \text{km}, 500\ \text{km})$—within the model C-SALT area. As expected, the newly generated steps are thin. Over the next few years they merge continuously (Figs. 10b,c), which decreases the number of layers and correspondingly increases the average step heights. The mergers ceased after 4 decades of model run when the staircase reached the steady state with a layer thickness of 20–50 m. The merging pattern is revealed most clearly by the space–time diagram of the temperature gradient in Fig. 11. In a striking illustration of pure B-merger dynamics, the interfaces remain spatially localized to near their original z levels. The ultimate demise of weak interfaces occurs through their gradual erosion, compensated by the strengthening of adjacent interfaces. These mergers have been attributed to the gamma effect—the variation of the flux ratio with the density ratio (Huppert 1971; Radko 2003, 2005). In Part II of this study, we shall investigate the mechanics of B

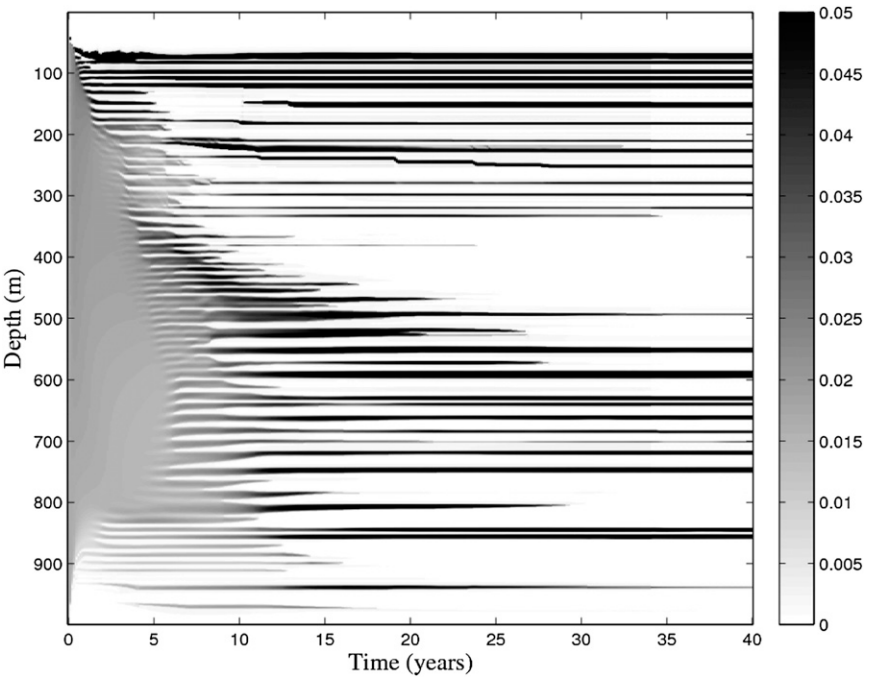

FIG. 11. Space–time diagram of the vertical temperature gradient at $(x, y) = (500\,\text{km}, 500\,\text{km})$. Layers merge when the relatively strong interfaces grow further at the expense of weaker interfaces that gradually decay and eventually disappear, following the B-merger scenario. The maximum gradient is $0.33°\text{C}\,\text{m}^{-1}$. The grayscale is used for the range $0° < T_z < 0.05°\text{C}\,\text{m}^{-1}$, and the data points with $T_z > 0.05°$ are shown in black.

mergers in greater detail, using a combination of analytical arguments, direct numerical simulations, and oceanographic observations. The consistency of the merging pattern in Fig. 11 with these results lends extra credence to both the parametric large-scale simulations of thermohaline layering (Part I) and the layer-merging theory (Part II).

6. Discussion

This study presents the first basin-scale staircase-resolving simulation, which is used to test earlier hypotheses for the origin of staircases. The key take-home message from this investigation is comforting: layering in large-scale simulations is largely controlled by one-dimensional dynamics. Earlier small-domain DNS (Radko 2003; Stellmach et al. 2011) and analytical models (Radko 2003, 2005) suggest that the staircases are caused by the gamma instability, associated with the variation of the flux ratio as a function of the density ratio. The present large-scale numerical model confirms this proposition. The gamma instability produces amplifying horizontal perturbations that eventually transform the vertical gradient into a series of well-mixed layers separated by high-gradient interfaces. The subsequent evolution of the model staircases is characterized by a series of merging events in which slightly weaker interfaces weaken further and eventually disappear without drifting vertically (the B-merger pattern). The merging dynamics are explored more systematically in Part II. The inclusion of multidimensional effects—associated with lateral background gradients, large-scale shears, and nonuniform stratification—has not led to major qualitative revisions of the gamma instability scenario.

Both the analytical theory (section 3) and the model runs (section 4) suggest that thermohaline layering is highly sensitive to the intensity of turbulent mixing, driven by overturning gravity waves. The increasing (decreasing) background turbulent diffusivity results in the contraction (expansion) of the area occupied by thermohaline staircases. Such sensitivity can be explored to infer the turbulent diffusivity based on the incidences of layering in the ocean. For instance, the Caribbean (C-SALT) staircase is characterized by $R_\rho < 1.7$. This condition requires turbulent diffusivity of $K^{\text{turb}} \sim 1.35 \times 10^{-6}\,\text{m}^2\,\text{s}^{-1}$, which is consistent with estimates of wave-induced mixing at the C-SALT latitude based on microstructure analysis and on finescale parameterizations.

The present study is only the first step in large-scale staircase-resolving modeling; a myriad of questions can

and will be addressed by such simulations in the future. For instance, staircase-resolving modeling is the most obvious tool that can be used to assess the impact of staircases on regional dynamics and on the global thermohaline circulation. Modeling can also help to generate essential insights into the problem of the spatial orientation of high-gradient interfaces—the processes controlling the slopes of interfaces relative to the slopes of isotherms and isohalines. The present simulations are limited in this regard by the crude lateral resolution of $\Delta x = \Delta y = 10^5$ m, which was adopted for computational feasibility reasons as a compensation for the required vertical resolution ($\Delta z = 1$ m). However, continuous developments in high-performance computing suggest that staircase-resolving models with much higher lateral resolution will be available in the not-too-distant future. The interaction of staircases with active mesoscale variability is an example of a problem that may soon be within the reach of models. Another set of intriguing effects is associated with the inclusion of pronounced lateral *T–S* fronts and resulting thermohaline interleaving on lateral scales of a few kilometers. These effects are not represented in the present simulations but will be in future high-resolution versions of the model. Nevertheless, even our initial success in staircase-resolving modeling is noteworthy and encouraging. It indicates that the progress in parameterizing double diffusion and in understanding the dynamics of layering has reached the level necessary to start producing consistent numerical models of thermohaline staircases.

Acknowledgments. The authors thank the editor Karen Heywood and the anonymous reviewers for helpful comments. Support of the National Science Foundation (Grants OCE 1334914, CBET 0933057, and ANT 0944536) is gratefully acknowledged. The computing resources for this project were supplied by the Extreme Science and Engineering Discovery Environment (XSEDE) program, which is supported by the National Science Foundation Grant OCI-1053575.

REFERENCES

Gregg, M. C., 1989: Scaling turbulent dissipation in the thermocline. *J. Geophys. Res.,* **94** (C7), 9686–9698, doi:10.1029/JC094iC07p09686.

Huppert, H. E., 1971: On the stability of a series of double-diffusive layers. *Deep-Sea Res. Oceanogr. Abstr.,* **18,** 1005–1021, doi:10.1016/0011-7471(71)90005-2.

Large, W. G., J. C. McWilliams, and S. C. Doney, 1994: Oceanic vertical mixing: A review and a model with a nonlocal boundary layer parameterization. *Rev. Geophys.,* **32,** 363–403, doi:10.1029/94RG01872.

Levitus, S., and T. P. Boyer, 1994: *Temperature.* Vol. 4, *World Ocean Atlas 1994,* NOAA Atlas NESDIS 4, 117 pp.

Luyten, J. R., J. Pedlosky, and H. Stommel, 1983: The ventilated thermocline. *J. Phys. Oceanogr.,* **13,** 292–309, doi:10.1175/1520-0485(1983)013<0292:TVT>2.0.CO;2.

Magnell, B., 1976: Salt fingers observed in the Mediterranean outflow region (34°N, 11°W) using a towed sensor. *J. Phys. Oceanogr.,* **6,** 511–523, doi:10.1175/1520-0485(1976)006<0511:SFOITM>2.0.CO;2.

Marshall, J., A. Adcroft, C. Hill, L. Perelman, and C. Heisey, 1997a: A finite-volume, incompressible Navier Stokes model for studies of the ocean on parallel computers. *J. Geophys. Res.,* **102** (C3), 5753–5766, doi:10.1029/96JC02775.

——, C. Hill, L. Perelman, and A. Adcroft, 1997b: Hydrostatic, quasi-hydrostatic, and nonhydrostatic ocean modeling. *J. Geophys. Res.,* **102** (C3), 5733–5752, doi:10.1029/96JC02776.

Merryfield, W. J., 2000: Origin of thermohaline staircases. *J. Phys. Oceanogr.,* **30,** 1046–1068, doi:10.1175/1520-0485(2000)030<1046:OOTS>2.0.CO;2.

——, G. Holloway, and A. E. Gargett, 1999: A global ocean model with double-diffusive mixing. *J. Phys. Oceanogr.,* **29,** 1124–1142, doi:10.1175/1520-0485(1999)029<1124:AGOMWD>2.0.CO;2.

Oschlies, A., H. Dietze, and P. Kahler, 2003: Salt-finger driven enhancement of upper ocean nutrient supply. *Geophys. Res. Lett.,* **30,** 2204, doi:10.1029/2003GL018552.

Polzin, K., J. M. Toole, and R. W. Schmitt, 1995: Finescale parameterizations of turbulent dissipation. *J. Phys. Oceanogr.,* **25,** 306–328, doi:10.1175/1520-0485(1995)025<0306:FPOTD>2.0.CO;2.

Radko, T., 2003: A mechanism for layer formation in a double-diffusive fluid. *J. Fluid Mech.,* **497,** 365–380, doi:10.1017/S0022112003006785.

——, 2005: What determines the thickness of layers in a thermohaline staircase? *J. Fluid Mech.,* **523,** 79–98, doi:10.1017/S0022112004002290.

——, 2007: Mechanics of merging event for a series of layers in a stratified turbulent fluid. *J. Fluid Mech.,* **577,** 251–273, doi:10.1017/S0022112007004703.

——, 2013: *Double-Diffusive Convection.* Cambridge University Press, 344 pp.

——, and D. P. Smith, 2012: Equilibrium transport in double-diffusive convection. *J. Fluid Mech.,* **692,** 5–27, doi:10.1017/jfm.2011.343.

——, J. Flanagan, S. Stellmach, and M.-L. Timmermans, 2014: Double-diffusive recipes. Part II: Layer-merging events. *J. Phys. Oceanogr.,* **44,** 1285–1305, doi:10.1175/JPO-D-13-0156.1.

Schmitt, R. W., 1979a: The growth rate of super-critical salt fingers. *Deep-Sea Res.,* **26A,** 23–40, doi:10.1016/0198-0149(79)90083-9.

——, 1979b: Flux measurements on salt fingers at an interface. *J. Mar. Res.,* **37,** 419–436.

——, H. Perkins, J. D. Boyd, and M. C. Stalcup, 1987: C-SALT: An investigation of the thermohaline staircase in the western tropical North Atlantic. *Deep-Sea Res.,* **34A,** 1655–1665, doi:10.1016/0198-0149(87)90014-8.

——, J. R. Ledwell, E. T. Montgomery, K. L. Polzin, and J. M. Toole, 2005: Enhanced diapycnal mixing by salt fingers in the thermocline of the tropical Atlantic. *Science,* **308,** 685–688, doi:10.1126/science.1108678.

Stellmach, S., A. Traxler, P. Garaud, N. Brummell, and T. Radko, 2011: Dynamics of fingering convection. Part 2: The formation of thermohaline staircases. *J. Fluid Mech.,* **677,** 554–571, doi:10.1017/jfm.2011.99.

Tait, R. I., and M. R. Howe, 1968: Some observations of thermo-haline stratification in the deep ocean. *Deep-Sea*

Res. Oceanogr. Abstr., **15,** 275–280, doi:10.1016/0011-7471(68)90005-3.

——, and ——, 1971: Thermohaline staircase. *Nature,* **231,** 178–179, doi:10.1038/231178a0.

Traxler, A., S. Stellmach, P. Garaud, T. Radko, and N. Brummel, 2011: Dynamics of fingering convection. Part 1: Small-scale fluxes and large-scale instabilities. *J. Fluid Mech.,* **677,** 530–553, doi:10.1017/jfm.2011.98.

Walsh, D., and B. R. Ruddick, 2000: Double-diffusive interleaving in the presence of turbulence: The effect of a nonconstant flux ratio. *J. Phys. Oceanogr.,* **30,** 2231–2245, doi:10.1175/1520-0485(2000)030<2231:DDIITP>2.0.CO;2.

Zhang, J., R. W. Schmitt, and R. X. Huang, 1998: Sensitivity of GFDL Modular Ocean Model to the parameterization of double-diffusive processes. *J. Phys. Oceanogr.,* **28,** 589–605, doi:10.1175/1520-0485(1998)028<0589:SOTGMO>2.0.CO;2.

Zodiatis, G., and G. P. Gasparini, 1996: Thermohaline staircase formations in the Tyrrhenian Sea. *Deep-Sea Res.,* **43,** 655–678, doi:10.1016/0967-0637(96)00032-5.